ORIGINAL ARTICLE

Eur. J. Anat. 20 (3): 195 - 203 (2016)

Anatomic study of the normal Bengal tiger (*Panthera tigris tigris*) brain and associated structures using low field magnetic resonance imaging

José Raduan Jaber[1], Mario Encinoso[2], Daniel Morales[1], Alejandro Artiles[2], Moisés Santana[1], Diego Blanco[1], Alberto Arencibia[1]

[1]*Department of Morphology, Faculty of Veterinary, University of Las Palmas de Gran Canaria, Canary Islands, Spain,* [2]*Veterinary Hospital Los Tarahales, Las Palmas de Gran Canaria, Spain*

SUMMARY

The aim of this paper was to study the brain and associated structures of the Bengal tiger's (*Panthera tigris tigris*) head by low-field magnetic resonance imaging (MRI). A cadaver of a mature female was used to perform spin-echo T1 and T2-weighting pulse sequences in sagittal, transverse and dorsal planes, using a magnet of 0.2 Tesla. Relevant anatomic structures were identified and labelled on the MRI according to the location and the characteristic signal intensity of different organic tissues. Spin-echo T1 and T2-weighted MR images were useful to demonstrate the anatomy of the brain and associated structures of the Bengal tiger's head. This study could enhance our understanding of normal brain anatomy in Bengal tigers.

Key words: MRI – Anatomy – Brain – Bengal tiger

INTRODUCTION

Veterinarians and wildlife researchers are involved in large feline conservation tasks that includes clinical, physiological and behavioural studies (Weissengruber et al., 2002; Bollo et al., 2011; Sajjad et al., 2011; Farooq et al*.,* 2012; Maas et al., 2013), as well as researches in order to better understand its normal anatomy (Khan, 2004; Mazák et al., 2011; Diogo et al., 2012). The application of modern diagnostic imaging techniques such as computed tomography (CT) or magnetic resonance imaging (MRI) have revolutionized the diagnostic imaging in feline medicine, being used sparingly for descriptive anatomical research (Hudson et al., 1995; Mogicato et al., 2012), as well as in diagnosing diseases of the head (Negrin et al., 2010; Gunn-Moore and Reed, 2011). Reports of MRI in large felines such as the Bengal tiger have been limited to the study of central infarction and haemorrhage (Snow et al., 2004), suspected neurotoxicity (Zeira et al., 2012) and normal anatomy of stifle joints (Arencibia et al., 2015). Although MRI was used to examine the Bengal tiger's brain (Snow et al., 2004), no detailed anatomical information has been described to date. The evaluation of the feline brain is particularly interesting due to its complex anatomy, and the different types of pathologies described such as neoplasia (Dietz et al., 1985; Kang et al., 2006) or head trauma (Ketz-Riley et al., 2004). Therefore, the purpose of this study was to provide an overview of the anatomy of the brain and associated structures of the Bengal tiger, using sagittal, transverse and dorsal MRI.

MATERIALS AND METHODS

Animals

A cadaver of 6-year-old female Bengal tiger

Corresponding author: Dr. José Raduán Jaber Mohamad. Department of Morphology, Faculty of Veterinary, University of Las Palmas de Gran Canaria, Canary Islands, Spain.
E-mail: joseraduan.jaber@ulpgc.es

Submitted: 26 January, 2016. *Accepted:* 14 April, 2016.

Table 1. Basic technical parameters used in this MRI study

	SE-T1-weighted	SE T2-weighted
Repetition time (ms)	Sagittal plane: 530 Transverse plane: 590 Dorsal plane: 500	Sagittal plane: 3520 Transverse plane: 3890 Dorsal plane: 3520
Echo time (ms)	Sagittal plane: 26 Transverse plane: 26 Dorsal plane: 26	Sagittal plane: 80 Transverse plane: 80 Dorsal plane: 80
Number of acquisitions	Sagittal plane: 4 Transverse plane: 4 Dorsal plane: 4	Sagittal plane: 2 Transverse plane: 2 Dorsal plane: 2
Slice thickness (mm)	Sagittal plane: 4 Transverse plane: 4.5 Dorsal plane: 4	Sagittal plane: 4 Transverse plane: 4.5 Dorsal plane: 4
Interslice spacing (mm)	Sagittal plane: 4.4 Transverse plane: 4.9 Dorsal plane: 4.4	Sagittal plane: 4.4 Transverse plane: 4.9 Dorsal plane: 4.4
Acquisition matrix	Sagittal plane: 256 X 256 Transverse plane: 256 X 256 Dorsal plane: 256 X 256	Sagittal plane: 256 X 256 Transverse plane: 256 X 256 Dorsal plane: 256 X 256

(*Panthera tigris tigris*) with a weight of 105 kg, born in captivity in Cocodrilos Park Zoo (Gran Canaria, Canary Islands, Spain) was used. This animal died of natural causes not related to head disorders. The study was conducted with the control of the Ethical Commission of Veterinary Medicine of the University of Las Palmas de Gran Canaria (agreement MV-2015/05).

MRI technique

The tiger was frozen immediately after death. Two days later, the cadaver was thawed during 48 hours to perform the MR study using a 0.2-Tesla magnet (Vet-MR Esaote, Genova, Italy) and a head coil. The animal was positioned in lateral recumbency during the MRI procedure. MR images were acquired by spin-echo pulse sequences (SE). T1 and T2-weighted MR images were obtained in sagittal, tranverse and dorsal planes. Basic technical parameters are presented in Table 1.

Anatomic evaluation

Anatomic details of the Bengal tiger’s brain and associated structures on the MR images were evaluated according to the characteristic signal intensity of the different bony components and soft -tissues structures. Identifiable anatomical structures were labelled with the aid of anatomical texts (Schaller and Constantinescu, 2007) and reports on feline MRI (Hudson et al., 1995; Snow et al., 2004; Mogicato et al., 2012). In addition, osseous preparations were used to facilitate accurate anatomic interpretation.

RESULTS

Nine representative MR images of the Bengal tiger’s head were selected. A midsaggital MR image is presented in Fig. 1. Transverse MR images are shown in a rostral to caudal progression from the level of the olfactory bulb to the myelencephalon, and oriented so that the left side of the head is to the viewer´s right and dorsal is at the top (Figs. 2-8). A dorsal MR image at the level of olfactory bulb and peduncle is presented in Fig. 9.

Spin-echo T1 and T2-weighted MRI of the tiger’s head provided adequate details of clinically relevant anatomical structures, showing good discrimination between soft and mineralized tissues. Therefore, bony structures such as the frontal bone (with their orbital part and squama), parietal, temporal (including the squamous, petrous and tympanic parts), the presphenoid bone (corpus and wing), the basisphenoid bone (body and wing) and the occipital bone (with their basilar and lateral parts, and squama) could be identified. These bony components could be visualized due to the fat that in the bone marrow appeared with intermediate signal intensity, as well as by the area of negligible signal corresponding to the cortical bone margins (Figs. 1-9). In addition, the lumen of air-filled structures such as frontal and sphenoidal sinuses (Figs. 1-4), tympanic bulla (Figs. 7-8), nasopharynx and oropharynx (Figs. 1-8) appeared with low signal intensity in the images, and were well differentiated by MRI.

Several parts of the encephalon such as the olfactory bulb and peduncles (Figs. 1-3 and 9), corpus callosum, fornix, internal capsule, optic chiasm, thalamus, hypothalamus, hypophysis, cavernous sinus, mesencephalon (including the mesencephalic tectum and cerebral peduncles), pons, myelencephalon, cerebral hemispheres and cerebellum (with their vermis and hemispheres), as well as the encephalic ventricular system could be

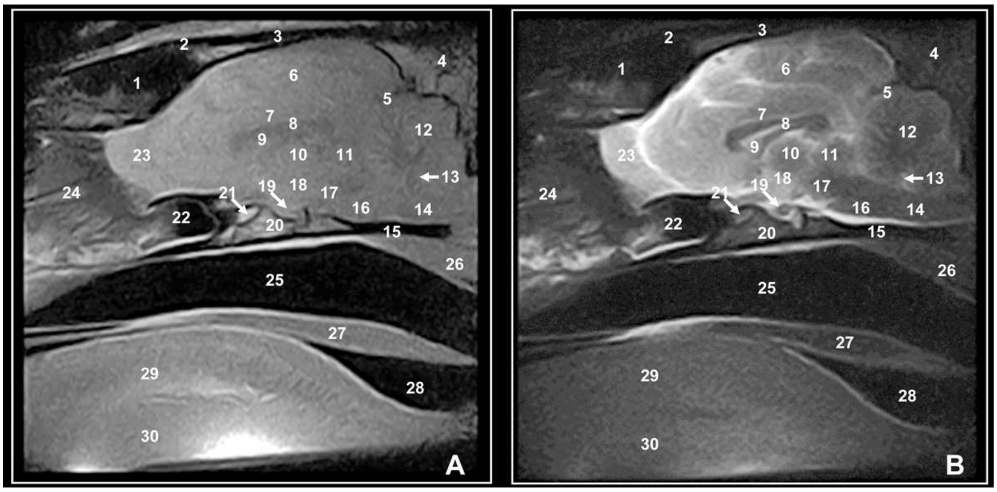

Fig. 1. (**A**) T1-weighted sagittal MR image and (**B**) T2-weighted sagittal MR image of a Bengal tiger's (*Panthera tigris*) brain. Left lateral aspect. 1. Frontal sinus; 2. Frontal bone; 3. Parietal bone; 4. Occipital squama; 5. Cerebral transverse fissure; 6. Cerebral hemisphere; 7. Corpus callosum; 8. Lateral ventricle; 9. Fornix; 10. Thalamus; 11. Mesencephalic tectum; 12. Cerebellar vermis; 13. Fourth ventricle; 14. Myelencephalon; 15. Basilar part of occipital bone; 16. Pons; 17. Cerebral peduncle; 18. Hypothalamus; 19. Hypophysis in the fossa hypophysialis of the basisphenoid bone; 20. Body of basisphenoid bone; 21. Optic chiasm; 22. Sphenoidal sinus; 23. Olfactory bulb; 24. Nasal cavity and labyrinthus ethmoidalis; 25. Nasopharynx; 26. Rectus ventralis and longus capitis muscles; 27. Soft palate; 28. Oropharynx; 29. Tongue; 30. Geniohyoid and genioglossus muscles.

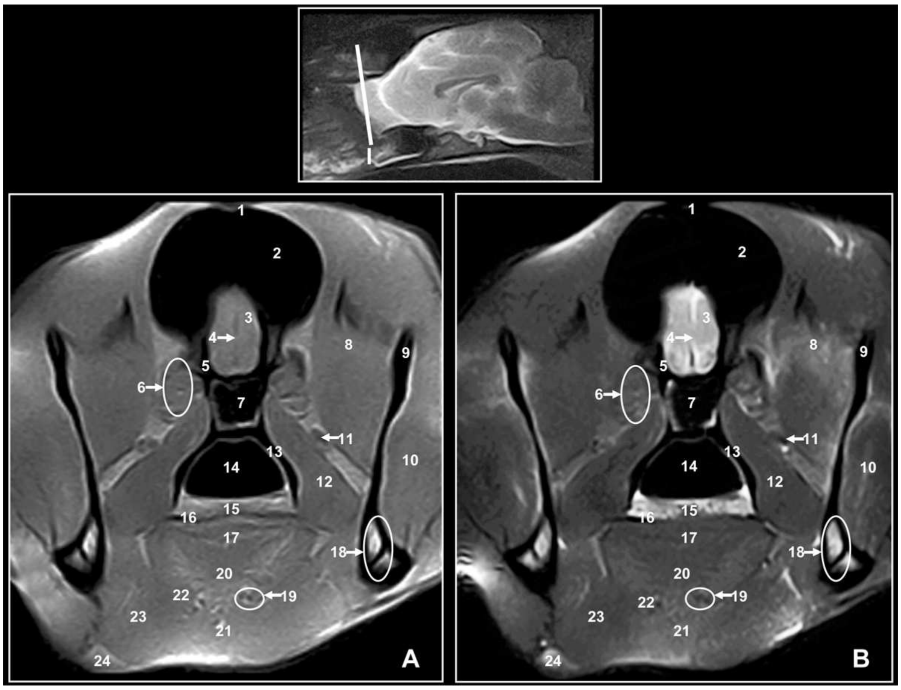

Fig. 2. (**A**) T1-weighted transverse MR image and (**B**) T2-weighted transverse MR image at the level of olfactory bulb (level I). Rostral aspect. 1. Frontal bone; 2. Frontal sinus; 3. Olfactory bulb; 4. Longitudinal cerebral fissure; 5. Wing of presphenoid bone; 6. Cavernous sinus and maxillary, trochlear, abducent and ophthalmic nerves; 7. Sphenoidal sinus; 8. Temporal muscle; 9. Ramus of mandible; 10. Masseter muscle; 11. Maxillary artery and nerve; 12. Medial pterygoid muscle; 13. Perpendicular plate of palatine bone; 14. Nasopharynx; 15. Soft palate; 16. Oral cavity; 17. Tongue; 18. Mandibular canal: inferior alveolar nerve, artery and vein; 19. Deep lingual artery and vein; 20. Genioglossus muscle; 21. Geniohyoid and mylohyoid muscles; 22. Styloglossus and hyoglossus muscles; 23. Digastric muscle; 24. Facial artery and vein.

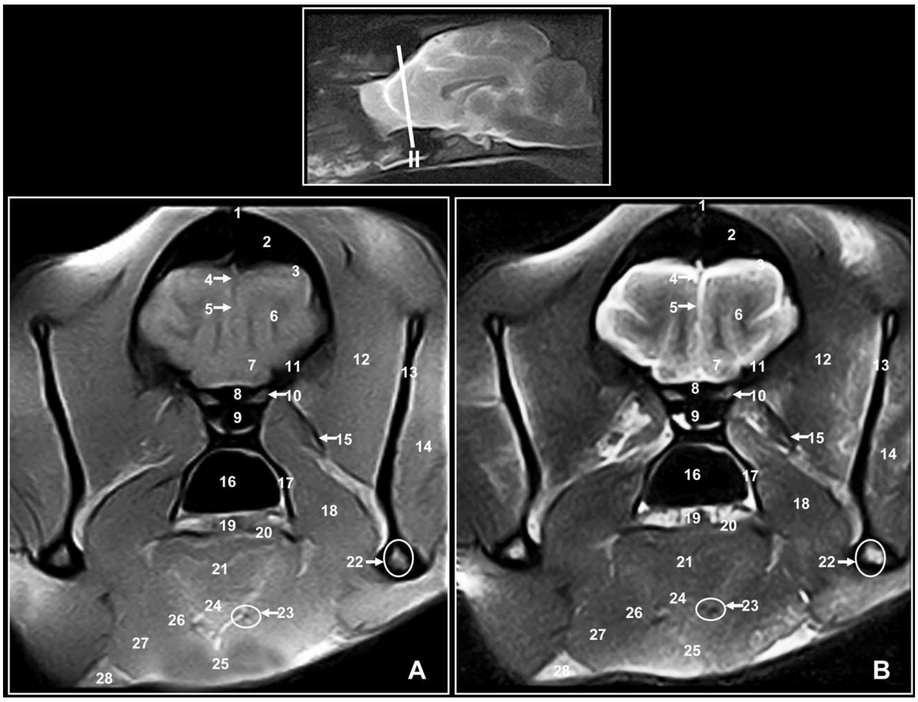

Fig. 3. (**A**) T1-weighted transverse MR image and (**B**) T2-weighted transverse MR image at the level of optic nerve (level II). Rostral aspect. 1. Frontal bone; 2. Frontal sinus; 3. Meninx of the brain; 4. Dorsal sagittal sinus; 5. Longitudinal cerebral fissure; 6. Cerebral hemisphere: frontal cortex; 7. Olfactory peduncle; 8. Jugum sphenoidale; 9. Sphenoidal sinus; 10. Optic nerve; 11. Wing of presphenoid bone; 12. Temporal muscle; 13. Ramus of mandible; 14. Masseter muscle; 15. Maxillary artery and nerve; 16. Nasopharynx; 17. Perpendicular plate of palatine bone; 18. Medial pterygoid muscle; 19. Soft palate; 20. Oral cavity; 21. Tongue; 22. Mandibular canal: inferior alveolar nerve, artery and vein; 23. Deep lingual artery and vein; 24. Genioglossus muscle; 25. Geniohyoid and mylohyoid muscles; 26. Styloglossus and hyoglossus muscles; 27. Digastric muscle; 28. Facial artery and vein.

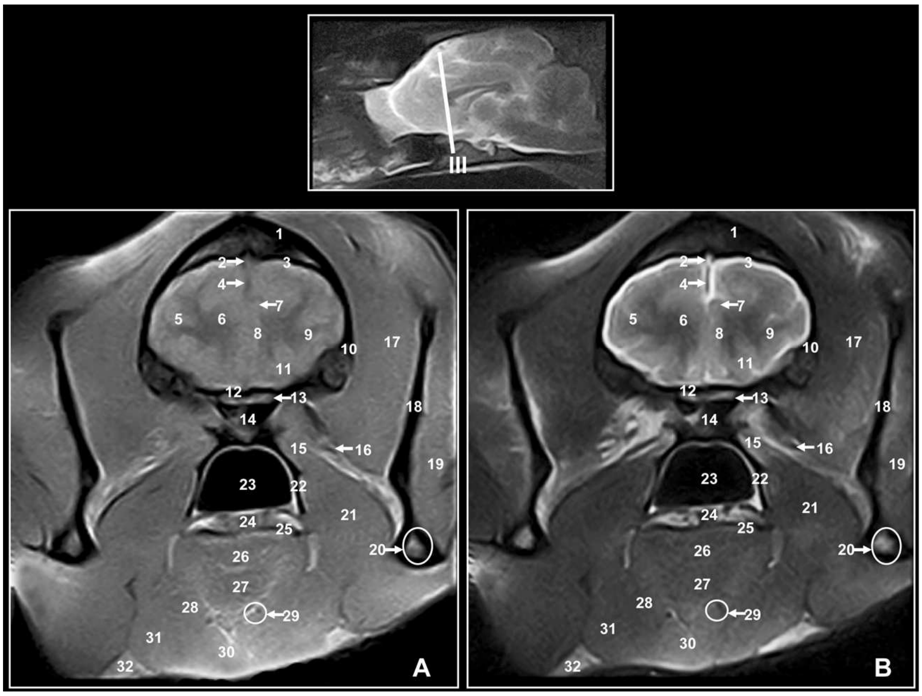

Fig. 4. (**A**) T1-weighted transverse MR image and (**B**) T2-weighted transverse MR image at the level of optic chiasm (level III). Rostral aspect. 1. Parietal bone; 2. Dorsal sagittal sinus; 3. Cavum subarachnoideale; 4. Cerebral longitudinal fissure; 5. Cerebral hemisphere; 6. Caudate nucleus; 7. Corpus callosum; 8. Fornix; 9. Internal capsule; 10. Squamous part of temporal bone; 11. Olfactory peduncle; 12. Jugum sphenoidale; 13. Optic chiasm; 14. Sphenoidal sinus; 15. Lateral pterygoid muscle; 16. Maxillary artery and nerve; 17. Temporal muscle; 18. Ramus of mandible; 19. Masseter muscle; 20. Mandibular canal: inferior alveolar nerve, artery and vein; 21. Medial pterygoid muscle; 22. Perpendicular plate of palatine bone; 23. Nasopharynx; 24. Soft palate; 25. Oral cavity; 26. Tongue; 27. Genioglossus muscle; 28. Styloglossus and hyoglossus muscles; 29. Deep lingual artery and vein. 30 = Geniohyoid and mylohyoid muscles. 31. Digastric muscle; 32 = Facial artery and vein.

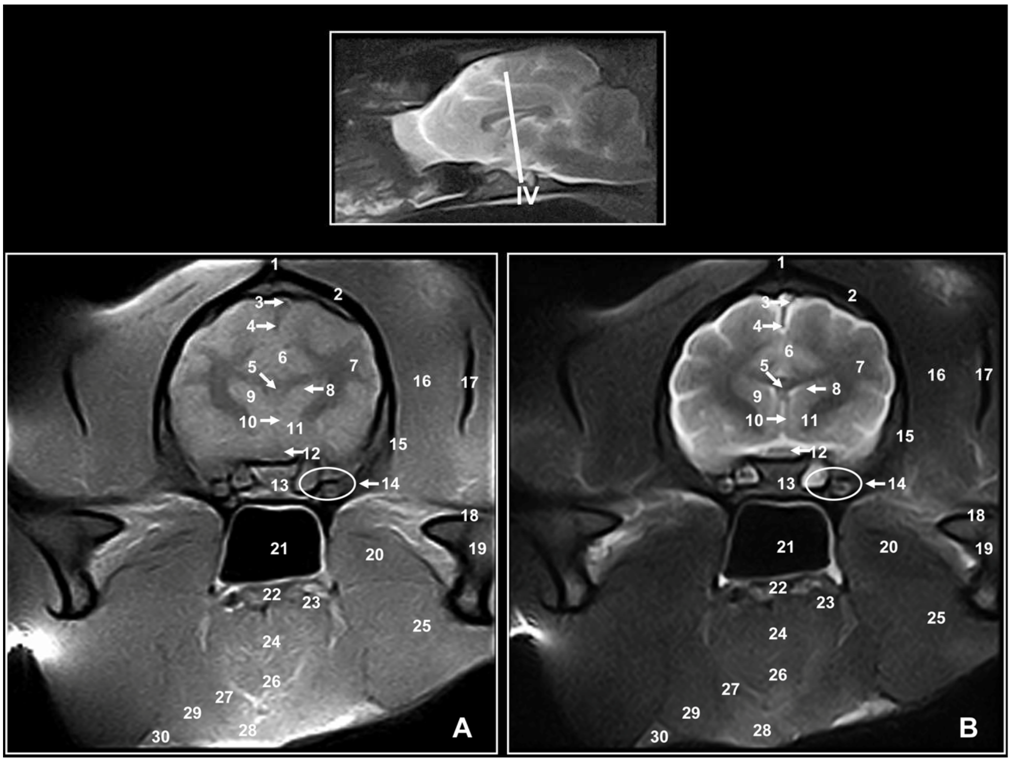

Fig. 5. (**A**) T1-weighted transverse MR image and (**B**) T2-weighted transverse MR image (**B**) at the level of thalamus and hypophysis (level IV). Rostral aspect. 1. External sagittal crest; 2. Parietal bone; 3. Dorsal sagittal sinus; 4. Cerebral longitudinal fissure; 5. Fornix; 6. Corpus callosum; 7. Corona radiata; 8. Lateral ventricle; 9. Thalamus; 10. Third ventricle; 11. Internal capsule; 12. Hypophysis; 13. Body of basisphenoid bone; 14. Cavernous sinus; 15. Squamous part of temporal bone; 16. Temporal muscle; 17. Coronoid process of mandible; 18. Temporomandibular joint: articular disc; 19. Condylar process of mandible; 20. Lateral pterygoid muscle; 21. Nasopharynx; 22. Soft palate; 23. Oropharynx; 24. Tongue; 25. Medial pterygoid muscle; 26. Genioglossus muscle; 27. Styloglossus and hyoglossus muscles; 28. Geniohyoid and mylohyoid muscles; 29. Digastric muscle; 30. Facial artery and vein.

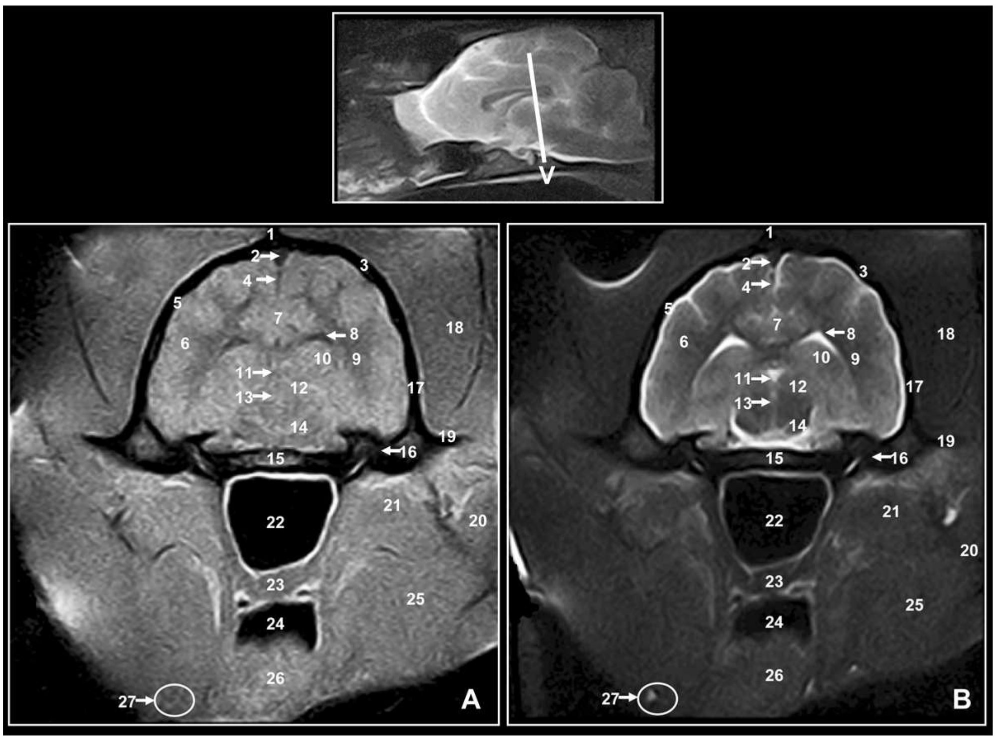

Fig. 6. (**A**) T1-weighted transverse MR image and (**B**) T2-weighted transverse MR image at the level of mesencephalon (level V). Rostral aspect. 1. External sagittal crest; 2. Dorsal sagittal sinus; 3. Parietal bone; 4. Cerebral longitudinal fissure; 5. Cavum subarachnoideale; 6. Cerebral hemisphere; 7. Corpus callosum; 8. Lateral ventricle (central part); 9. Lateral ventricle (temporal horn); 10. Hippocampus; 11. Third ventricle; 12. Mesencephalic tectum; 13. Mesencephalic aqueduct. 14. Cerebral peduncle; 15. Body of basisphenoid bone; 16. Wing of basisphenoid bone; 17. Squamous part of temporal bone; 18. Temporal muscle; 19. Zygomatic process of temporal bone; 20. Masseter muscle; 21. Lateral pterygoid muscle; 22. Nasopharynx; 23. Soft palate; 24. Oropharynx; 25. Medial pterygoid muscle; 26. Geniohyoid and mylohyoid muscles; 27. Facial artery and vein.

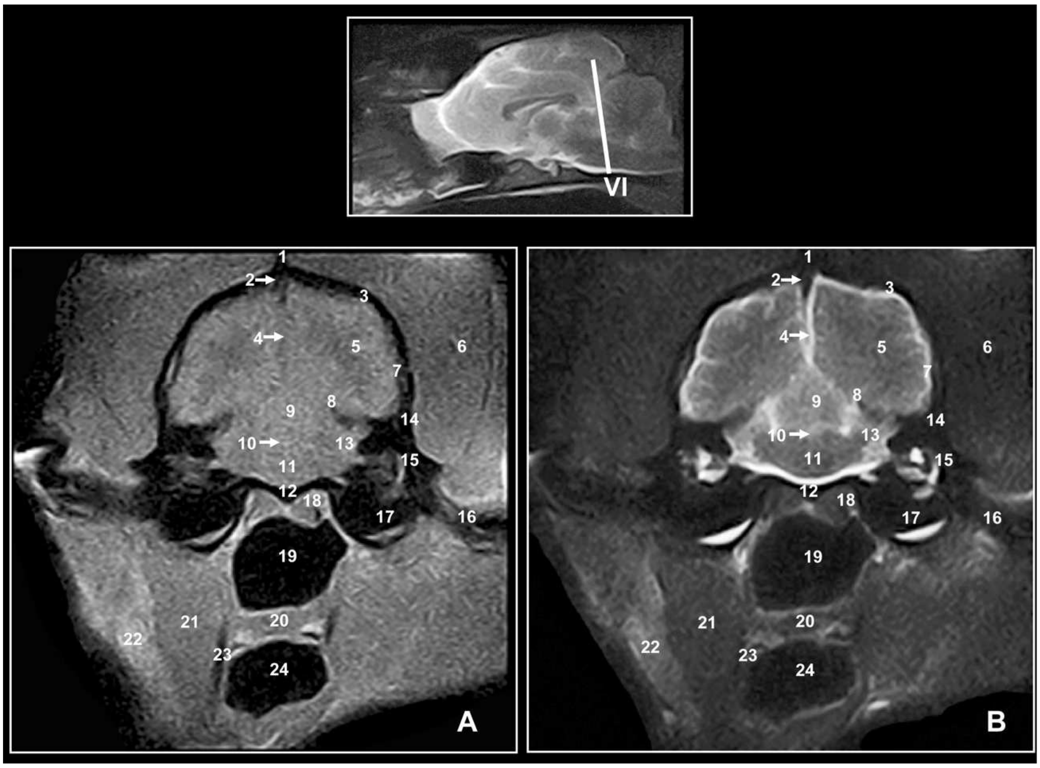

Fig. 7. (**A**) T1-weighted transverse MR image and (**B**) T2-weighted transverse MR image at the level of pons (level VI). Rostral aspect. 1. External sagittal crest; 2. Dorsal sagittal sinus; 3. Parietal bone; 4. Cerebral longitudinal fissure; 5. Cerebral hemisphere; 6. Temporal muscle; 7. Cavum subarachnoideale; 8. Cerebral transverse fissure; 9. Cerebellum: rostral lobe; 10. Fourth ventricle; 11. Pons; 12. Basilar part of occipital bone; 13. Cerebellar hemisphere; 14. Squamous part of temporal bone; 15. Petrous part of temporal bone; 16. External acoustic meatus; 17. Tympanic part of temporal bone; 18. Rectus ventralis and longus capitis muscles; 19. Nasopharynx; 20. Soft palate; 21. Digastric muscle; 22. Parotid gland; 23. Hyoid bone; 24. Oropharynx.

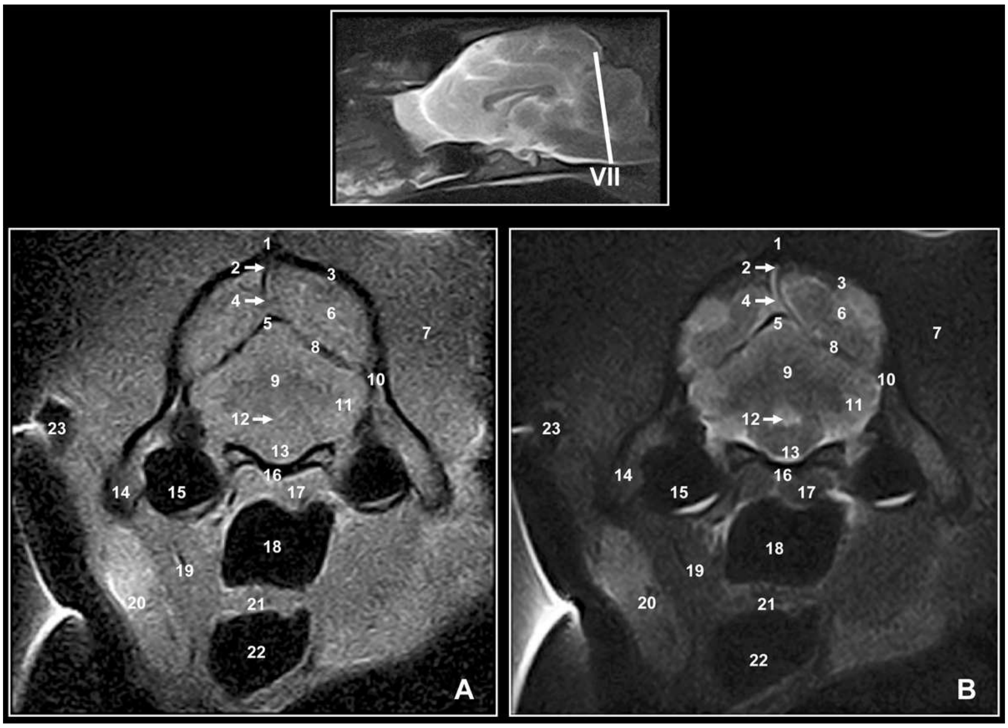

Fig. 8. T1-weighted transverse MR image (**A**) and T2-weighted transverse MR image (**B**) at the level of myelencephalon (level VII). Rostral aspect. 1. External sagittal crest; 2. Dorsal sagittal sinus; 3. Parietal bone; 4. Cerebral longitudinal fissure; 5. Cerebellar tentorium; 6. Cerebral hemisphere; 7. Temporal muscle; 8. Transverse cerebral fissure; 9. Cerebellar vermis; 10. Squamous part of temporal bone; 11. Cerebellar hemisphere; 12. Fourth ventricle; 13. Myelencephalon; 14. Paracondylar process of occipital bone; 15. Tympanic bulla; 16. Basilar part of occipital bone; 17. Rectus ventralis and longus capitis muscles; 18. Nasopharynx; 19. Digastric muscle; 20. Parotid gland; 21. Soft palate; 22. Oropharynx; 23. Auricular cavity.

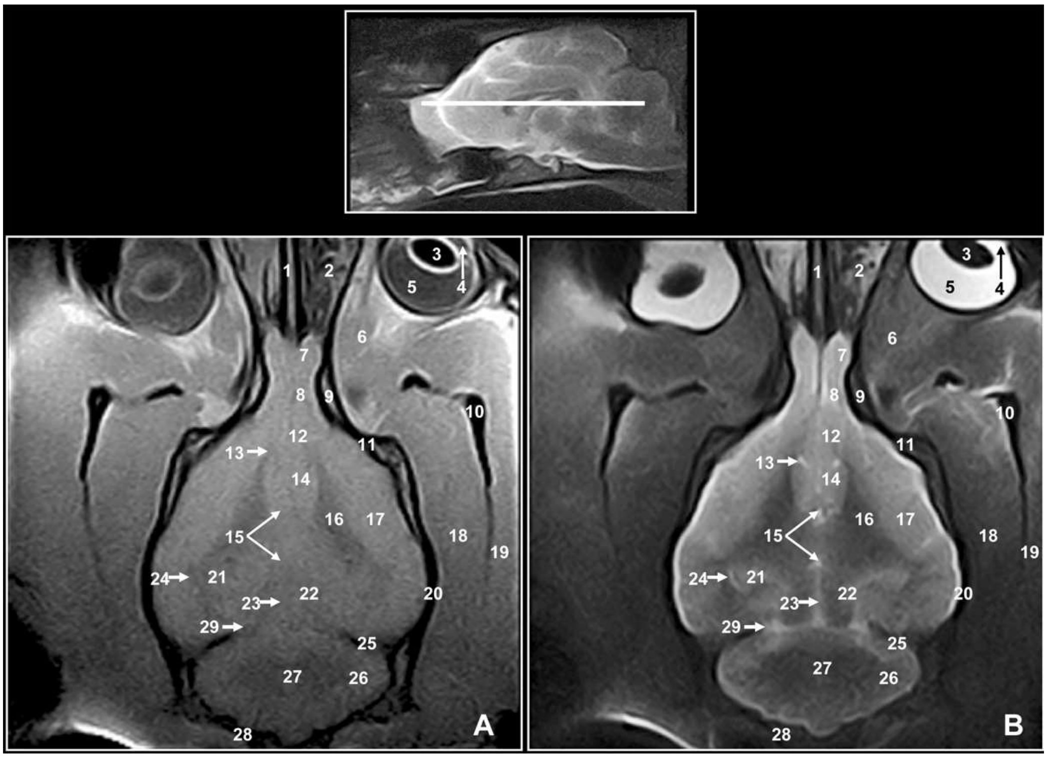

Fig. 9. T1-weighted dorsal MR image (**A**) and T2-weighted dorsal MR image (**B**) at the level of the mesencephalon and thalamus. Dorsal aspect. 1. Cartilage of the nasal septum; 2. Labyrinthus ethmoidalis; 3. Lens; 4. Anterior chamber of eyeball; 5. Vitreous chamber of eyeball; 6. Eyeball muscles; 7. Olfactory bulb; 8. Olfactory peduncle; 9. Orbit; 10. Coronoid process of mandible; 11. Frontal bone; 12. Rostral comissure; 13. Lateral ventricle: frontal horn; 14. Caudatus nucleus; 15. Third ventricle (intethalamic adhesion is between arrows); 16. Internal capsule; 17. Cerebral hemisphere; 18. Medial pterygoid muscle; 19. Temporal muscle; 20. Parietal bone; 21. Hippocampus; 22. Mesencephalic collicules; 23. Mesencephalic aqueduct; 24. Lateral ventricle: temporal horn; 25. Cerebral transverse fissure; 26. Cerebellar hemisphere; 27. Cerebellar vermis; 28. Occipital squama; 29. Lateral recess of fourth ventricle.

identified on MR images (Figs. 1 and 3-9). Cerebrospinal fluid from the subarachnoid space and the cerebral ventricles appeared with low signal intensity (dark gray) on the T1-weighted MR images. However, in T2-weighted images, this fluid appeared with high signal intensity (white).

Associated structures of the head such as the eyeball with the lens, as well as anterior and vitreous chambers were also identified. The aqueous and the vitreous humors appeared with low signal intensity in T1-weighted MR images and with high signal intensity in T2-weighted MR images. Lens appeared with low signal intensity in both MR images, whereas the capsule was better identified in T1 compared to T2 weighted MR images (Fig. 9).

DISCUSSION

Evaluation of anatomic structures of the Bengal tiger's head is laborious because of an anatomical complexity that makes difficult to diagnose morphological changes by means of physical examination and conventional radiographic studies. Moreover, the use and comparison of cadaver sections with diagnostic images in endangered species is difficult due to the fact that these animals are under very stricted regulations .

In large felines, contemporary image-based diagnostic techniques such as CT and MRI made possible to obtain images of body sections from different anatomic planes, with good anatomic resolution, high contrast between various structures, and excellent tissue differentiation (Snow et al., 2004; Zeira et al., 2012; Dziallas et al., 2012). Similar results were obtained in our work, where low-field MRI unit with head coil clearly delineated each anatomical portion of the tiger's brain and associated structures of the head. In comparison with other conventional image-based techniques, MRI allows discriminating between soft tissues and fluids of the feline head particularly well (Hudson et al., 1995; Snow et al., 2004; Mogicato et al., 2012). On the other hand, its use in endangered species is justified by the amount of diagnostic information obtained with little risk to the animals evaluated (Snow et al., 2004; Zeira et al., 2012).

In our study, low-field MRI of the tiger's head showed good spatial and contrast resolution of the different brain regions such as the cerebrum, cerebellum, and brain stem, mainly in T2-weighted MR images. Similar results were observed in the central nervous system of small felines (Yamada et al., 1995) and dogs (Snellman et al., 1999), using low-field strength. However, due to the nature of the low-field MRI and the size of the tiger head, some of the anatomical structures of the caudal part of encephalon were not clearly defined in T1 weighted images. Low-field (0.2-0.4T) MRI unit predominates in veterinary practice (Konar and Lang, 2011) due to their reduced costs compared to high-field MRI unit (Hayashi et al., 2004). Adequate quality examinations can be achieved using appropriate protocols and investing more scanning time than with high-field systems. The main disadvantage of low-field MR equipment is the reduced signal to noise ratio compared with high field systems, where higher signal-to-noise ratio results in improved imaging (Konar and Lang, 2011; Gray-Edwards et al., 2014), but recent technological developments of low-field MR units will lead to higher image quality, shorter scan times, and refined imaging protocols (Hayashi et al., 2004; Konar and Lang, 2011).

In our study , spin-echo T1 and T2-weighted MRI of the Bengal tiger's head provided good discrimination between the cranial bones, the encephalic tissues and associated structures of the head. Contrast between gray and white matter was higher in T2-weighted images, compared with T1-weighted images. Similar results were observed in other studies using spin-echo pulse pulse sequences (Leigh et al., 2008; Mogicato et al., 2012). Most of the studies in domestic animals were imaged in sagittal, transverse and dorsal planes, showing relevant brain structures (Leigh et al., 2008; Conchou et al., 2012; Mogicato et al., 2012). In the present study, similar planes were used and allowed good differentiation of the anatomic structures on the median aspect (sagittal plane), the anatomic relationships of the cerebral structures (transverse plane), as well as adequate assesment of the encephalon (dorsal plane). The parameters (repetition time, echo time, number of acquisitions, section thickness, interslice spacing and acquisition matrix) utilized in this study could be used as a valid reference for exploratory evaluation of the Bengal tiger's brain and associated structures.

The application of MRI in large feline medicine is currently limited because of its expense, availability, and the logistic problems of acquiring MR images. With developing technology, including new developments in open magnet design, MR imaging could become more readily available for tiger imaging. Future MRI studies of this kind of endangered species should be examined and discussed with a higher Tesla device.

In conclussion, MRI using spin-echo pulse sequence (T1 and T2-weighted images) provided adequate anatomical details of the tiger head and its associated structures that could be used as initial reference in future anatomical, functional and clinical studies of this region.

ACKNOWLEDGEMENTS

This work was supported by funds of the Department of Morphology of Las Palmas de Gran Canaria University (Spain).

REFERENCES

ARENCIBIA A, ENCINOSO M, JABER JR, MORALES D, BLANCO D, ARTILES A, VÁZQUEZ JM (2015) Magnetic resonance imaging study in a normal Bengal Tiger (*Panthera Tigris*) stifle joint. *BMC Vet Res*, 11: 192.

BOLLO E, SCAGLIONE FE, TURSI M, SCHRÖDER C, DEGIORGI G, BELLUSO E, CAPELLA S, BELLIS D (2011) Malignant pleural mesothelioma in a female Lion (*Panthera Leo*). *Res Vet Sci*, 91: 116-118.

CONCHOU F, SAUTET J, RAHARISON F, MOGICATO G (2012) Magnetic resonance imaging of normal nasal cavity and paranasal sinuses in cats. *Anat Histol Embryol*, 41: 60-67.

DIETZ HH, ERIKSEN E, JENSEN AO (1985) Coloboma of the optic nerve head in Bengal tiger kittens (*Panthera Tigris Tigris*). *Acta Vet Scand*, 26: 136-139.

DIOGO R, PASTOR F, DE PAZ F, POTAU JM, BELLO-HELLEGOUARCH G, FERRERO EM, FISHER RE (2012) The head and neck muscles of the serval and tiger: homologies, evolution, and proposal of mammalian and veterinary muscle ontology. *Anat Rec*, 295: 2157-2178.

DZIALLAS P, BECKER A, BÖSING B, ZIMMERING T, BÖER M, MISCHKE R, KÄSTNER S, WEFSTAEDT P, NOLTE I (2012) Computed tomography diagnostic of a retrobulbar abscess in a white tiger. *Tierarztl Prax Ausg K Kleintiere Heimtiere*, 40: 59-63.

FAROOQ U, SAJJAD S, ANWAR M, KHAN BN (2012) Serum chemistry variables of Bengal Tigers (*Panthera tigris tigris*) kept in various forms of captivity. *Pak Vet J*, 32: 283-285.

GRAY-EDWARDS HL, SALIBI N, JOSEPHSON EM, HUDSON JA, COX NR, RANDLE AN, McCURDY VJ, BRADBURY AN, WILSON DU, BEYERS RJ, DENNEY TS, MARTIN DR (2014) High resolution MRI anatomy of the cat brain at 3-Tesla. *J Neurosci Methods*, 30: 10-17.

GUNN-MOORE DA, REED N (2011) CNS disease in the cat: current knowledge of infectious causes. *J Feline Med Surg*, 13: 824-836.

HAYASHI N, WATANABE Y, MASUMOTO T, MORI H, AOKI S, OHTOMO K, OKITSU O, TAKAHASHI T (2004) Utilization of low-field MR scanners. *Magn Reson Med Sci*, 3: 27-38.

HUDSON LC, CAUZINILLE L, KORNEGAY JN (1995) Magnetic resonance imaging of the normal feline brain. *Vet Radiol Ultrasound*, 37: 267-275.

KANG MS, PARK MS, KWON SW, MA SA, CHO DY, KIM DY, KIM Y (2006) Amyloid-producing odontogenic tumour (calcifiying epithelial odontogenic tumour) in the mandible of a Bengal tiger (*Pantera Tigris Tigris*). *J Comp Pathol*, 134: 236-240.

KETZ-RILEY CJ, GALLOWAY DS, HOOVER JP, ROCHAT MC, BAHR RJ, RITCHEY JW, CAUDELL DL (2004) Paresis secondary to an extradural hematoma in a Sumatran tiger (*Panthera tigris sumatrae*). *J Zoo Wildl Med*, 35: 208-215.

KHAN MMH (2004) Ecology and Conservation of the Bengal Tiger in the Sundarbans Mangrove Forest of Bangladesh. Department of Anatomy, University of Cambridge, Cambridge.

KONAR M, LANG J (2011) Pros and cons of low-field magnetic resonance imaging in veterinary practice. *Vet Radiol Ultrasound*, 52: S5-S14.

MAAS M, KEET DF, NIELEN M (2013) Hematologic and serum chemistry reference intervals for free-ranging lions (*Panthera Leo*). *Res Vet Sci*, 95: 266-268.

MAZÁK JH, CHRISTIANSEN P, KITHCHENER AC (2011) Oldest known pantherine skull and evolution of the tiger. *PLoS ONE*, 6: e25483.

MOGICATO G, CONCHOU F, LAYSSOL-LAMOUR C, RAHARISON F, SAUTET J (2012) Normal feline brain: clinical anatomy using magnetic resonance imaging. *Anat Histol Embryol,* 41: 87-95.

NEGRIN A, CHERUBINI GB, LAMB C, BENIGNI L, ADAMS V, PLATT S (2010) Clinical signs, magnetic resonance imaging findings and outcome in 77 cats with vestibular disease: a retrospective study. *J Feline Med Surg,* 12: 291-299.

LEIGH EJ, MACKILLOP E, ROBERTSON ID, HUDSON LC (2008) Clinical anatomy of the canine brain using magnetic resonance imaging. *Vet Radiol Ultrasound*, 49: 113-121.

SAJJAD S, FAROOQ U, ANWAR M, KHURSHID A, SA BUKHARI SA (2011) Effect of captive environment on plasma cortisol level and behavioral pattern of Bengal tigers (*Panthera tigris tigris*). *Pak Vet J*, 31: 195-198.

SCHALLER O, CONSTANTINESCU GM (2007) *Illustrated Veterinary Anatomical Nomenclature*. 2nd ed. Enke Verlag, Sttutgart.

SNELLMAN M, BENCZIK J, JOENSUU R, RAMADAN UA, TANTTU J, SAVOLAINEN S (1999) Low-field magnetic resonance imaging of beagle brain with a dedicated receiver coil. *Vet Radiol Ultrasound*, 40: 36-39.

SNOW TM, LITSTER AL, GREGORY RJW, HANGER JJ (2004) Big cat scan: Magnetic resonance imaging of the tiger. *Australas Radiol*, 48: 93-95.

WEISSENGRUBER GE, FORSTENPOINTER G, PETERS G, KÜBBER-HEISS A, FITCH WY (2002) Hyoid apparatus and pharynx in the lion (*Panthera leo*), jaguar (*Panthera onca*), tiger (*Panthera tigris*), cheetah (*Acinonyxjubatus*) and domestic cat (*Felis silvestris f. catus*). *J Anat*, 201: 195-209.

YAMADA K, MIYAHARA K, SATO M, HIROSE T, YASUGI Y, MATSUDA Y, FURUHAMA K (1995) Magnetic resonance imaging of the central nervous system in the kitten. *J Vet Med Sci*, 57: 155-156.

ZEIRA O, BRIOLA C, KONAR M, DUMAS MP, WRZOSEK MA, PAPA V (2012) Suspected neurotoxicity due to clostridium perfringens type B in a tiger (*Panthera tigris*). *J Zoo Wildl Med*, 43: 666-669.